IBRO Neuroscience Reports 17 (2024) 138–144

Contents lists available at ScienceDirect

IBRO Neuroscience Reports

journal homepage: www.sciencedirect.com/journal/IBRO-Neuroscience-Reports

Research paper

Retinal inputs that drive optomotor responses of mice under mesopic conditions

CL Barta [a], WB Thoreson [a,b,*]

[a] Truhlsen Eye Institute and Department of Ophthalmology and Visual Sciences, USA
[b] Pharmacology and Experimental Neuroscience, University of Nebraska Medical Center, Omaha, NE 68198, USA

ARTICLE INFO

Keywords:
Optomotor response
Synaptotagmin
Rod photoreceptor cell
Ribbon synapse
Retina

ABSTRACT

Optomotor responses are a popular way to assess sub-cortical visual responses in mice. We studied photoreceptor inputs into optomotor circuits using genetically-modified mice lacking the exocytotic calcium sensors synaptotagmin 1 (Syt1) and 7 (Syt7) in rods or cones. We also tested mice that in which cone transducin, GNAT2, had been eliminated. We studied spatial frequency sensitivity under mesopic conditions by varying the spatial frequency of a grating rotating at 12 deg/s and contrast sensitivity by varying luminance contrast of 0.2c/deg gratings. We found that eliminating Syt1 from rods reduced responses to a low spatial frequency grating (0.05c/deg) consistent with low resolution in this pathway. Conversely, eliminating the ability of cones to respond to light (by eliminating GNAT2) or transmit light responses (by selectively eliminating Syt1) showed weaker responses to a high spatial frequency grating (3c/deg). Eliminating Syt7 from the entire optomotor pathway in a global knockout had no significant effect on optomotor responses. We isolated the secondary rod pathway involving transmission of rod responses to cones via gap junctions by simultaneously eliminating Syt1 from rods and GNAT2 from cones. We found that the secondary rod pathway is sufficient to drive robust optomotor responses under mesopic conditions. Finally, eliminating Syt1 from both rods and cones almost completely abolished optomotor responses, but we detected weak responses to large, bright rotating gratings that are likely driven by input from intrinsically photosensitive retinal ganglion cells.

Introduction

Optomotor head movements of mice and other species supplement optokinetic eye movements in providing visual stabilization (Kretschmer et al., 2017). Head movements are easier to detect than eye movements in mice and so optomotor responses have become a popular way to assess sub-cortical visual responses in this widely used experimental animal (Abdeljalil et al., 2005; Leinonen and Tanila, 2018; Prusky et al., 2004; Umino et al., 2008). A number of studies have explored photoreceptor inputs into optomotor pathways by using mutant mice in which rods and/or cones are incapable of generating light responses, but many of these models also exhibit retinal degeneration (Milla-Navarro et al., 2022; Schmucker et al., 2005; Schroeder et al., 2018; Umino et al., 2008). In this study, we took advantage of genetically-modified mouse lines for selective elimination of exocytotic calcium sensors from rods or cones, eliminating synaptic release while retaining the capability for light responses.

Like many other neurons, the main calcium sensor used by both rods and cones is synaptotagmin 1 (Syt1) (Grassmeyer et al., 2019; Mesnard et al., 2022). Eliminating Syt1 from cones is sufficient to abolish photopic b-waves as well as responses to high frequency flicker, showing that Syt1 is the sole sensor used by cones. Eliminating Syt1 from both rods and cones abolished scotopic b-waves (Grassmeyer et al., 2019; Mesnard et al., 2022) and abolished responses of retinal ganglion cells evoked by optogenetic stimulation of channelrhodopsin expressed in photoreceptors (Sladek and Thoreson, 2023). Although loss of Syt1 is sufficient to abolish light-driven responses in downstream neurons, the high affinity sensor, Syt7, is also present in rods (Mesnard et al., 2022). In whole cell recordings of rods, eliminating Syt7 from rods selectively reduced glutamate release evoked by long depolarizing steps whereas eliminating Syt1 abolished release evoked by short steps. However, eliminating Syt7 by itself from rods had no effect on ERG b-waves and eliminating Syt7 from rods and cones that lacked Syt1 did not depress ERG b-waves further. The effects of Syt7 in rods could only be detected

* Correspondence to: Department of Ophthalmology and Visual Sciences, Durham Research Center 1, University of Nebraska Medical Center, Omaha, NE 68198-5840, USA.
E-mail address: wbthores@unmc.edu (W. Thoreson).

https://doi.org/10.1016/j.ibneur.2024.07.003
Received 5 March 2024; Received in revised form 11 July 2024; Accepted 20 July 2024
Available online 21 July 2024

under non-physiological conditions such as strong and maintained depolarization or the absence of Syt1, suggesting Syt7 only plays a complementary role in regulating light-driven changes in glutamate release from photoreceptors. Consistent with limited contributions from Syt7, we show here that global elimination of Syt7 had no effect on optomotor responses. In the absence of any effect of eliminating Syt7 in a global knockout, these data further suggests that this sensor has little role in the entire optomotor circuit.

Output from rods reaches the inner retina through at least three different pathways (Fain and Sampath, 2018; Grimes et al., 2018). The primary pathway operating under scotopic conditions is the connection from rods to rod bipolar cells. At higher intensities, a second pathway emerges whereby rod signals are conveyed through Cx36 gap junctions to cones and from there to cone bipolar cells. A third pathway involving direct contacts between rods and OFF-type bipolar cells emerges at still brighter intensities. Eliminating Syt1 from rods selectively eliminates the primary and tertiary pathways, leaving only the secondary pathway intact. Our results showed that transmission of rod signals to cones via gap junctions is sufficient to drive robust optomotor responses under mesopic conditions. Finally, we saw weak responses to large, bright rotating gratings in mice entirely lacking synaptic output from both rods and cones, suggesting that these residual responses are driven by intrinsically photosensitive retinal ganglion cells.

Materials and methods

Mice

We used control C57Bl6J and mutant mice of both sexes aged 4–8 weeks for these experiments. $Syt1^{flox}$ (Syt1: MGI:99667) and $Syt7^{flox}$ mice were generated by the UNMC Genome Engineering Core as described previously (Grassmeyer et al., 2019; Mesnard et al., 2022; Quadros et al., 2017). Yun Le (Univ. of Oklahoma) generously provided HRGP-Cre mice. $Syt7^{flox}$ mice were created on C56Bl6J background. $Syt1^{flox}$ were originally generated on C57Bl6N background and HRGP-Cre created in FVB/N mice. Both of these mouse lines were then back-crossed into C57Bl6J. Rho-iCre mice were obtained from Jackson Laboratories, Bar Harbor, ME (B6.Cg-Pde6b+ Tg(Rho-iCre)1Ck/Boc; RRID: 015850) where they are maintained on C57Bl6J background. Rho-iCre and HRGP-Cre mice selectively express cre-recombinase in rods and cones, respectively (Le et al., 2004; Li et al., 2005). To eliminate Syt1 and Syt7 selectively from rods and cones, we crossed Rho-iCre and HRGP-Cre mouse lines with $Syt1^{fl/fl}$ and $Syt7^{fl/fl}$ mice. CMV-Cre mice were obtained from Jackson Laboratories (B6.C-Tg(CMV-cre) 1Cgn/J). These mice produce ubiquitous expression of cre-recombinase under control of a minimal human cytomegalovirus promoter. We bred $Syt7^{fl/fl}$ with CMV-Cre mice to generate global Syt7 knockouts (Syt7 KO). GNAT2 KO mice on C57Bl6J background were generously provided by Marie Burns (University of California –Davis) (Ronning et al., 2018). The absence of cone transducin GNAT2 in these mice eliminates cone light responses but they retain normal cone anatomy and do not exhibit retinal degeneration (Ronning et al., 2018).

In accordance with AVMA Guidelines for the Euthanasia of Animals, euthanasia was performed by CO_2 asphyxiation followed by cervical dislocation. All animal care and handling protocols were approved by the University of Nebraska Medical Center Institutional Animal Care and Use Committee.

Optomotor assay

Chamber design

The visual function assay chamber was fabricated with interior dimensions of 54 ×54 x 32 cm (W x D x H) and a floor covered with mirrored glass. A circular platform (diameter=5 cm) was elevated 16 cm above the chamber floor. Four LCD monitors (Dell P2419H; 60 Hz refresh rate) were fitted into slots fabricated around the chamber. Each monitor subtended 90 deg x 58.1 deg visual angle with a pixel resolution of 18.5 pixels per degree with respect to the platform center. A camera (Allied Vision Mako G-158B; 60 Hz frame rate) was mounted 17.5 cm above the circular platform, providing 71.1 deg x 54.4 deg field of view with a pixel resolution of 20.4 pixels per degree. Camera and displays were controlled by MATLAB (R2019a; MathWorks) installed on a Windows PC (Dell OptiPlex 5060; Intel Core i7–8700 CPU @ 3.2 GHz; 32 GB RAM; NVIDIA Quadro M2000 GPU).

Stimulus design

Visual stimuli were generated and presented using the Visual Psychophysics Toolbox. Stimuli were comprised of vertical square wave gratings with spatial frequency manipulated to induce the illusion of a virtual cylinder with identical spatial frequency across the entire display. There was a slight discontinuity in phase at the junction of the video monitors when using the lowest spatial frequency (0.025c/deg; see Video). This phase discontinuity was not evident at higher spatial frequencies. Stimulus velocity was fixed at 12 degrees/second across all study procedures. This speed is optimal for eliciting optomotor responses (Umino et al., 2008). Spatial frequency sensitivity was assessed by presenting 100 % contrast gratings at 9 spatial frequencies (cycles/degree): 0.025, 0.05, 0.10, 0.20, 0.30, 0.35, 0.375, 0.40, and 0.45. Contrast sensitivity was assessed by presenting 0.20 cycles/degree gratings with following luminance contrasts ($C = (L_{max} - L_{min}) / L_{min}$): 0.01, 0.02, 0.04, 0.08, 0.16, 0.32, 0.64, and 0.96. Luminance was measured with a luminance meter (Konica Minolta LS-150).

Procedures

All animals were tested between 8:00 AM – 1:00 PM in a dimly lit room with ambient illumination of 2.4 cd/m^2 (mesopic). Mice were dark-adapted overnight prior to testing. No more than 8 animals were tested within a single day. Prior to stimulus presentation, animals were placed on the elevated circular platform and allowed to acclimate for at least 5 minutes (2.4 cd/m^2). Acclimation periods were terminated when gross movements in body positioned were minimized. Stimulus presentation procedures for each trial were as follows. Each trial began with a 2 second blank display (5.7 cd/m^2). Next, a static square wave grating of predetermined spatial frequency and contrast was presented for 0.33 seconds. Following the static display, the grating began moving to the left or right; initial stimulus direction was randomly determined. Stimulus motion lasted for 10 seconds and stimulus direction reversed halfway through the stimulus motion period. A blank inter-trial interval of 30 seconds (5.7 cd/m^2) followed each stimulus motion sequence. There were 9 and 16 total trials in the spatial frequency and contrast sensitivity protocols, respectively. Testing for each mouse took no longer than 30 minutes to complete.

Data processing

Videos underwent manual and automated processing. Manual processing routines were performed using custom MATLAB software and involved trained personnel counting the number of frames during which animals head movements appeared slow and reflexive– as opposed to more rapid and volitional – and moved in the same direction as the stimulus. During video analysis, mice were identified by number, not genotype. As a test for inter-observer variability, we had a second observer analyze a subset of mice and saw no significant differences between data from the two observers. Tracking performance was calculated as the percentage of counted frames relative to total stimulus movement frames.

Statistical analysis

Statistical analysis and data visualization were done using ClampFit 10 (Molecular Devices) and GraphPad Prism 9 software. Roughly equal numbers of male and female mice were used for these experiments. P-values were adjusted for multiple comparisons using the Holm-Sidak method. Error bars in the figures show SEM.

Results

Fig. 1 compares visual behavior in control C57Bl6J mice with mice lacking Syt1 and/or Syt7 in rods. Spatial frequency sensitivity was assessed from the optomotor response to a high contrast grating at various spatial frequency gratings rotating at 12 deg/s. The mean intensity of 2.4 cd/m^2 is within the mesopic range. Loss of synaptic output from rods by eliminating Syt1 (Rod^{Syt1CKO}, p=0.0012) or by eliminating both Syt1 and Syt7 (Rod^{Syt1Syt7CKO}, p=0.004) significantly reduced responses to a low spatial frequency grating of 0.05c/deg. Eliminating Syt1 and Syt7 together also reduced responses at 0.3c/deg (p=0.029) but loss of Syt1 alone did not produce a statistically significant reduction at this spatial frequency. There was no significant difference between the performance of mice lacking both Syt1 and Syt7 vs. mice lacking only Syt1 at any of the spatial frequencies that were tested. The weaker responses to 0.05c/deg in the absence of synaptic output from rods are consistent with studies showing that rods are more important for lower acuity vision than high acuity (Zele and Cao, 2014).

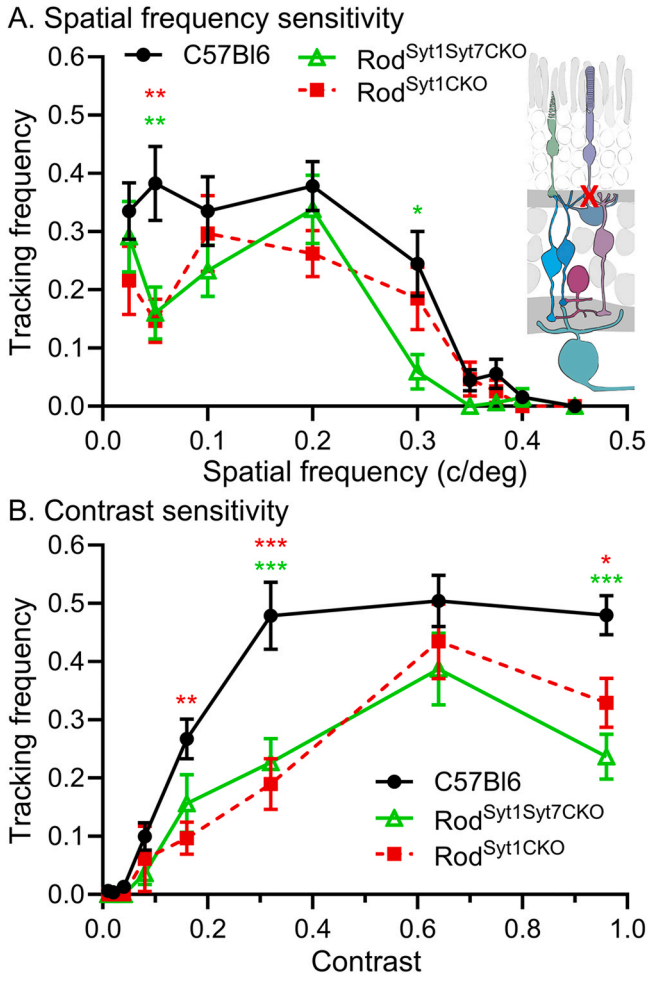

Fig. 1. Contributions of synaptic output from rods to optomotor responses in mice. A. Spatial frequency sensitivity was measured by varying the spatial frequency of a grating rotating at 12 deg/s with a mean intensity of 2.4 cd/m^2. Spatial frequency sensitivity was reduced significantly at 0.05c/deg in both Rod^{Syt1CKO} (n=12, p=0.0012, **) and Rod^{Syt1Syt7CKO} (n=10, p=0.004, **) mice. Rod^{Syt1Syt7CKO} mice also showed weaker responses at 0.3c/deg (p=0.029, *). B. Contrast sensitivity was assessed by varying the luminance contrast of 0.2c/deg gratings rotating at 12 deg/s. Tracking frequency was reduced in Rod^{Syt1CKO} mice at 0.16 (p=0.0056, **), 0.32 (p<0.0001, ***) and 0.96 (p=0.017, *) contrast. Tracking was also significantly reduced in Rod^{Syt1Syt7CKO} mice at contrasts of 0.32 (p<0.0001, ***) and 0.96 (p<0.0001, ***). Control C57Bl6, n=18 mice.

Contrast sensitivity was assessed by varying the luminance contrast of 0.2c/deg gratings rotating at 12 deg/s. Eliminating synaptic output from rods had a larger effect on contrast sensitivity than spatial frequency sensitivity. Tracking frequency was reduced from control (n=18 mice) at contrasts of 0.16 (p=0.0056), 0.32 (p<0.0001) and 0.96 (p=0.017) by loss of Syt1 alone (Rod^{Syt1CKO} mice, n=12). Loss of both Syt1 and Syt7 in Rod^{Syt1Syt7CKO} mice (n=10) caused statistically significant reductions at contrasts of 0.32 (p<0.0001) and 0.96 (p<0.0001).

Although these conditions should be virtually identical, tracking at 0.2c/deg with 0.96 contrast in the contrast sensitivity trials was better than tracking at 0.2c/deg in spatial frequency trials (p=0.047, paired t-test). The reason is not clear. Spatial frequency tests were performed before contrast sensitivity tests and so perhaps mice were more focused on the task by the time the latter trials were conducted.

As shown above, there were some subtle differences in optomotor responses between mice lacking only Syt1 or lacking both Syt1 and Syt7 from rods, but these small differences might simply be due to experimental variability. To test the importance of Syt7 for visual behavior in isolation, we generated mice that lacked this sensor entirely by crossing Syt7$^{fl/fl}$ mice with CMV-Cre mice that produce ubiquitous expression of cre-recombinase. The resulting Syt7 KO mice (n=15) showed no significant differences in either spatial frequency sensitivity or contrast sensitivity, despite the absence of Syt7 throughout all of the sensory and motor pathways engaged during optomotor responses (Fig. 2).

Eliminating Syt1 from cones is sufficient to abolish their synaptic output (Grassmeyer et al., 2019; Mesnard et al., 2022). Unlike Rod^{Syt1CKO} mice that showed weaker responses at a low spatial frequency, Cone^{Syt1CKO} mice (n=15) showed weaker responses at a higher spatial frequency of 0.3c/deg (p=0.0044). We also examined responses of GNAT2KO mice that lack cone alpha-transducin (Ronning et al., 2018), making their cones incapable of responding to light. Like Cone^{Syt1CKO} mice, GNAT2KO mice (n=11) showed weaker responses to 0.3c/deg grating (p=0.0047). However, like Rod^{Syt1CKO} mice, they also showed weaker responses at 0.05c/deg (p=0.0478). Cone^{Syt1CKO} mice showed better tracking at 0.2c/deg than GNAT2KO mice (p=0.0029). However, while they differed from one another, responses of Cone^{Syt1CKO} and GNAT2KO mice did not differ from control at this spatial frequency suggesting this difference might arise from experimental variability.

Contrast sensitivity was diminished across much of the contrast range in both Cone^{Syt1CKO} (n=15; 0.16, p = 0.0047; 0.32, p<0.0001; 0.64, p<0.0001; 0.96, p=0.0144) and GNAT2KO (n=11; 0.32, p<0.0001; 0.64, p<0.0001; 0.96, p=0.0072) mice. These data are consistent with contributions from both rods and cones to shaping contrast sensitivity under mesopic conditions.

We next analyzed GNAT2 KO mice that also lacked Syt1 in their rods. In these animals, rods can respond to light but are incapable of synaptic release. This eliminates both the primary rod-to-rod bipolar and tertiary rod-to-cone OFF bipolar cell pathways. We assumed that because GNAT2 KO cones retain their normal structure, they are likely capable of release and so the secondary rod pathway should remain intact. Rod^{Syt1CKO}/GNAT2KO mice (n=5) retained good spatial frequency sensitivity that was comparable to control mice, with only slightly weaker responses at 0.3c/deg (p=0.04, unpaired t-test; this difference was not significant when corrected for multiple comparisons due to the smaller number of Rod^{Syt1CKO}/GNAT2KO mice; n=5). This was similar to results with GNAT2KO mice that retain intact rod synapses. Contrast sensitivity of Rod^{Syt1CKO}/GNAT2 KO mice was diminished somewhat but differed significantly from control only at 0.32 contrast (p = 0.0028).

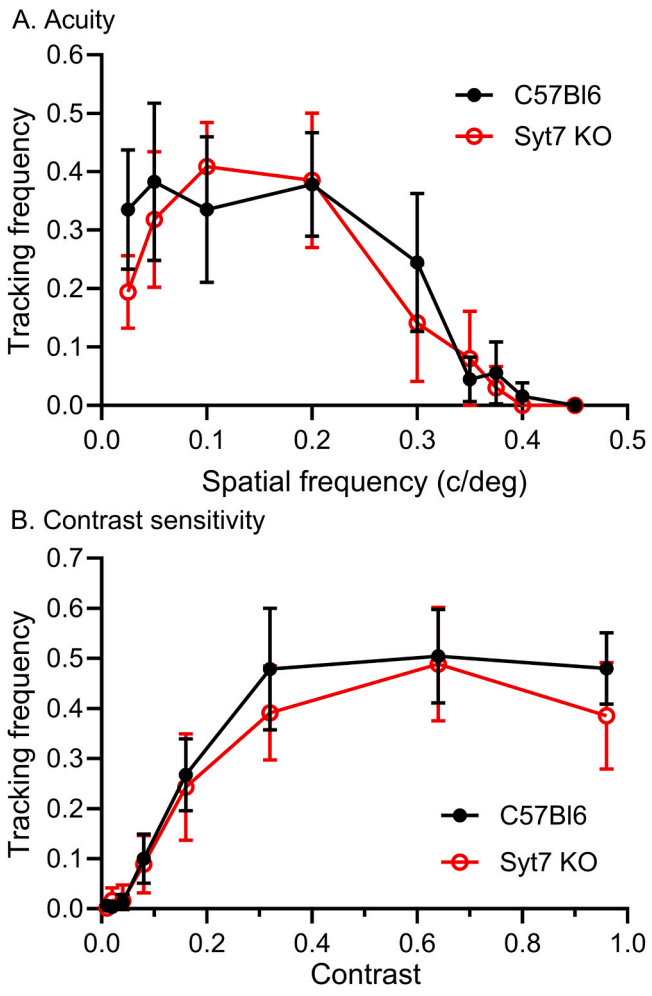

Fig. 2. Global elimination of Syt7 from mice had no significant effect on optomotor responses. A. Spatial frequency sensitivity. B. Contrast sensitivity. Syt7 KO, n=15 mice. C57Bl6, n=18 mice.

We tested mice that lack Syt1 in both rods and cones (Rod/Cone^{Syt1CKO}; n=13). Mice lacking Syt1 in rods and cones show no ERG b-wave and additional elimination of Syt7 has no significant further effect on the ERG (Mesnard et al., 2022), suggesting that Syt1 is the sole Ca^{2+} sensor that regulates light-evoked changes in synaptic output from both rods and cones. Responses to the 0.2c/deg grating used for testing contrast sensitivity were abolished in Rod/Cone^{Syt1CKO} mice, as well as in two mice lacking both Syt1 and Syt7 in rods and cones (Rod/Cone$^{Syt1/Syt7CKO}$). Loss of Syt1 from both rods and cones in Rod/Cone^{Syt1CKO} mice also significantly reduced tracking at all spatial frequencies: 0.05c/deg (p=0.012), 0.1c/deg (p=0.012), 0.2c/deg (p=0.008), and 0.3c/deg (<0.0001). However, we were surprised to find that Rod/Cone^{Syt1CKO} mice occasionally responded to low spatial frequency gratings (0.025–0.1c/deg). We illustrate this with a video of a mouse that fixates and then appears to track the 0.025c/deg grating. The same video shows behavior of a control C57Bl6 mouse responding to the same coarse grating. As shown in the video, control mice would occasionally fixate and briefly track the grating, but did so more often than Rod/Cone^{Syt1CKO} mice. To test if Syt7 might mediate these residual responses, we tested two Rod/Cone$^{Syt1/Syt7CKO}$ mice that lacked both Ca^{2+} sensors. These mice also showed occasional responses to gratings at the two lowest spatial frequencies suggesting that the visual inputs that drive this weak behavior originate elsewhere than rods and cones. The most likely candidates are intrinsically photosensitive retinal ganglion cells (Aranda and Schmidt, 2021; Brown et al., 2012; Flood et al., 2022; Lucas et al., 2020).

Discussion

Consistent with earlier work using mice that lacked rod or cone light responses, we showed that output from rods is more important for detecting low spatial frequency gratings whereas cone output is more important for high spatial frequency gratings (Schmucker et al., 2005). In addition, we showed that under mesopic conditions significant output can enter optomotor circuits via the secondary rod pathway in which signals travel from rods to cones via gap junctions. Finally, we saw weak responses to large bright gratings in mice where synaptic output from both rods and cones had been completely eliminated, suggesting that these responses are driven by output from ipRGCs.

Schmucker et al. (Schmucker et al., 2005) found that mice lacking cones showed optomotor responses similar to wild type mice and that eliminating rods reduced responses to higher spatial frequency gratings. Similarly, we saw that eliminating Syt1 from cones reduced tracking at 0.3c/deg whereas eliminating Syt1 from rods reduced responses at a low spatial frequency of 0.05c/deg. GNAT2KO mice lacking cone light responses also showed weaker responses to 0.3c/deg gratings supporting the idea that cones are primarily responsible for supporting visual responses at this higher spatial frequency under mesopic conditions. The significant decrease in responses of mice lacking Syt1 in rods at 0.05c/deg is consistent with lower resolution in the rod pathway, even in mice that lack a fovea.

Cone^{Syt1CKO} mice showed significantly greater tracking at 0.2c/deg than GNAT2KO mice. However, this may be due to experimental variability, since this condition is similar to contrast sensitivity measurements performed at 0.96 contrast where we did not see a similar difference.

Sensitivity was reduced at contrasts of 0.32 and above by eliminating cone light responses in GNAT2KO mice and by eliminating synaptic release in mice lacking Syt1 in cones. Cones in Cone^{Syt1CKO} mice can respond to light and so could theoretically transmit cone light responses via gap junctions into rods (in the opposite direction of the secondary rod pathway). However, this seems unlikely since both GNAT2KO and Cone^{Syt1CKO} mice showed a similar reduction in contrast sensitivity.

Rod^{Syt1CKO} mice showed reduced sensitivity to contrasts of 0.26, 0.34, and 0.96, but not 0.64. These mice retain cone light responses as well as the ability of cones to transmit rod responses via the secondary pathway (rod-cone gap junctions). GNAT2KO mice crossed with Rod^{Syt1CKO} mice retain only rod responses transmitted via the secondary pathway. C57Bl6J mice show deficits in melatonin production, hindering circadian control of gap junctional coupling (Doyle et al., 2002). While photopic illumination fully uncouples rods and cones (Jin and Ribelayga, 2016), rod input can reach cones via gap junctions under mesopic conditions (Jin et al., 2022) GNAT2KO/Rod^{Syt1CKO} mice that retain only the secondary rod pathway showed good contrast sensitivity, with a significant decrease only at 0.3c/deg. Using a two-alternative forced choice paradigm, Pasquale et al. (Pasquale et al., 2020) found evidence for a Cx36-independent pathway operating under mesopic conditions. GNAT2KO/Rod^{Syt1CKO} showed weaker tracking than control mice at 0.3c/deg, but this was also true of GNAT2KO and Cone^{Syt1CKO} mice so this deficit more likely reflects weaker cone output. Thus, while other pathways may contribute, our results suggest that the secondary rod pathway can support the transmission of contrast information under mesopic conditions.

We were surprised to see weak responses to rotating gratings in mice that lacked Syt1 in both rods and cones, as well as in mice lacking both Syt1 and Syt7 in photoreceptors. These responses were only seen with bright, low spatial frequency gratings. As illustrated in the video, mice lacking synaptic output from rods and cones would occasionally fixate on the stimulus and then appear to track its motion. The most likely candidates mediating these responses are intrinsically photosensitive retinal ganglion cells (Allen et al., 2017; Lucas et al., 2020; Schroeder et al., 2018). Consistent with this is a complete loss of optomotor responses in *Opn4*$^{-/-}$ × *Pde6b*$^{rd10/rd10}$ mice (Milla-Navarro et al., 2022).

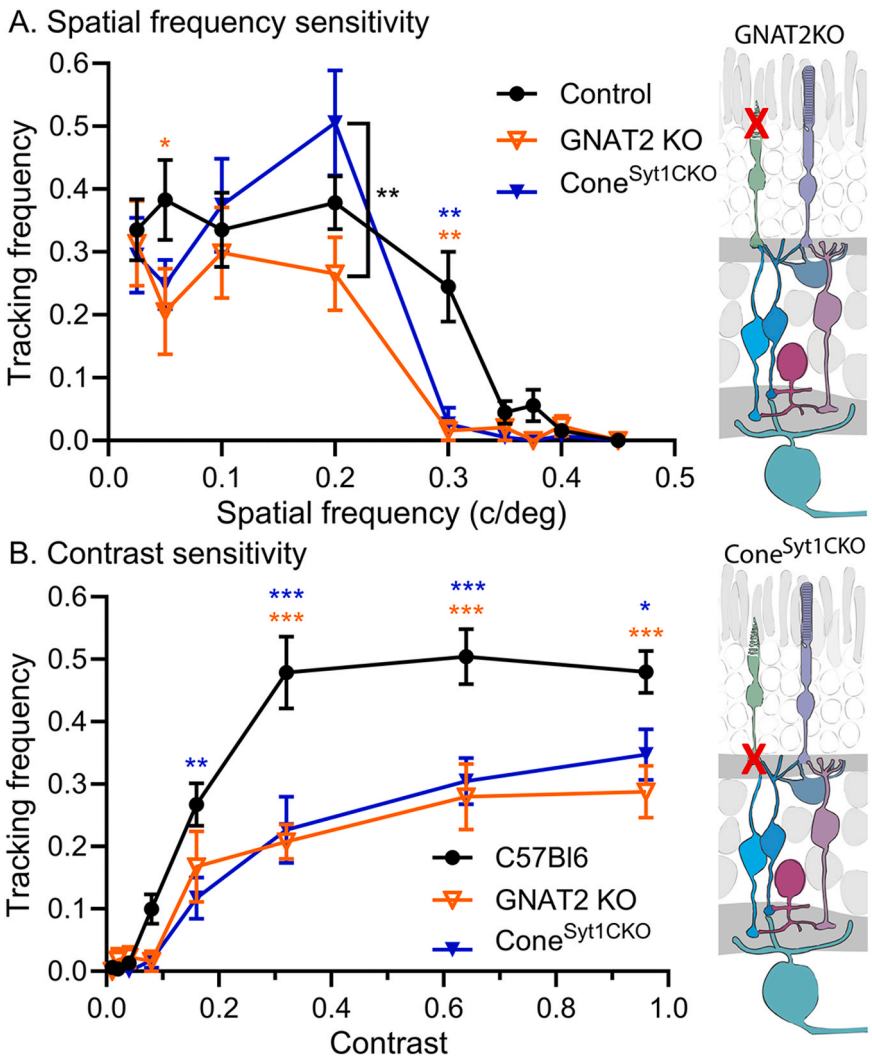

Fig. 3. Cone contributions to optomotor responses. A. Spatial frequency sensitivity. Cone^{Syt1CKO} mice (n=15) showed a significant reduction in sensitivity at 0.3c/deg (p=0.0044, **). GNAT2KO mice (n=11) showed weaker responses to 0.05c/deg (P=0.0478, *) and 0.3c/deg gratings (p=0.0047, **). Cone^{Syt1CKO} mice showed greater tracking at 0.2c/deg than GNAT2KO mice (p=0.0029, **). B. Contrast sensitivity was diminished in both Cone^{Syt1CKO} (0.16, p = 0.0047, **; 0.32, p<0.0001, ***; 0.64, p<0.0001, ***; 0.96, p=0.0144, *) and GNAT2 KO mice (0.32, p<0.0001, ***; 0.64, p<0.0001, ***; 0.96, p=0.0072, **).

Optomotor and optokinetic responses both rely on input from ON-direction selective ganglion cells into the accessory optic system (Aung et al., 2022; Kretschmer et al., 2017; Orhan et al., 2021; Oyster et al., 1980; Oyster et al., 1972; Pinto et al., 2007) with responses in the horizontal plane specifically involving input into the nucleus of the optic tract (NOT) (Robinson, 2022). While the NOT receives direct input from melanopsin-positive, intrinsically photosensitive retinal ganglion cells (Delwig et al., 2016), ipRGCs do not show direction-selective responses (Zhao et al., 2014) and their slow kinetics seem inconsistent with requirements for tracking a moving grating (Procyk et al., 2015; Schroeder et al., 2018; Walch et al., 2015). However, ipRGCs show robust responses to motion as well as strong projections to superior colliculus (Delwig et al., 2016; Ecker et al., 2010; Gooley et al., 2003; Zhao et al., 2014). Thus, while the Rod/Cone^{Syt1CKO} mouse in this video appears to track the grating, it is possible that this behavior simply reflects an awareness of visual motion and not true optomotor reflex responses. These data add to the increasing appreciation that visual information from ipRGCs can reach different brain regions to influence a variety of visual behaviors (Lucas et al., 2020).

Ethical approval

All animal care and handling protocols were approved by the University of Nebraska Medical Center Institutional Animal Care and Use Committee.

Consent to Publish

Both authors reviewed and approved the manuscript.

Funding

Supported by NIH grants EY10542, EY32396.

CRediT authorship contribution statement

Cody Barta: Investigation, analysis, editing. Wallace Thoreson: Conceptualization, analysis, writing, funding acquisition.

Declaration of Competing Interest

The authors have no conflicts of interest to declare regarding the

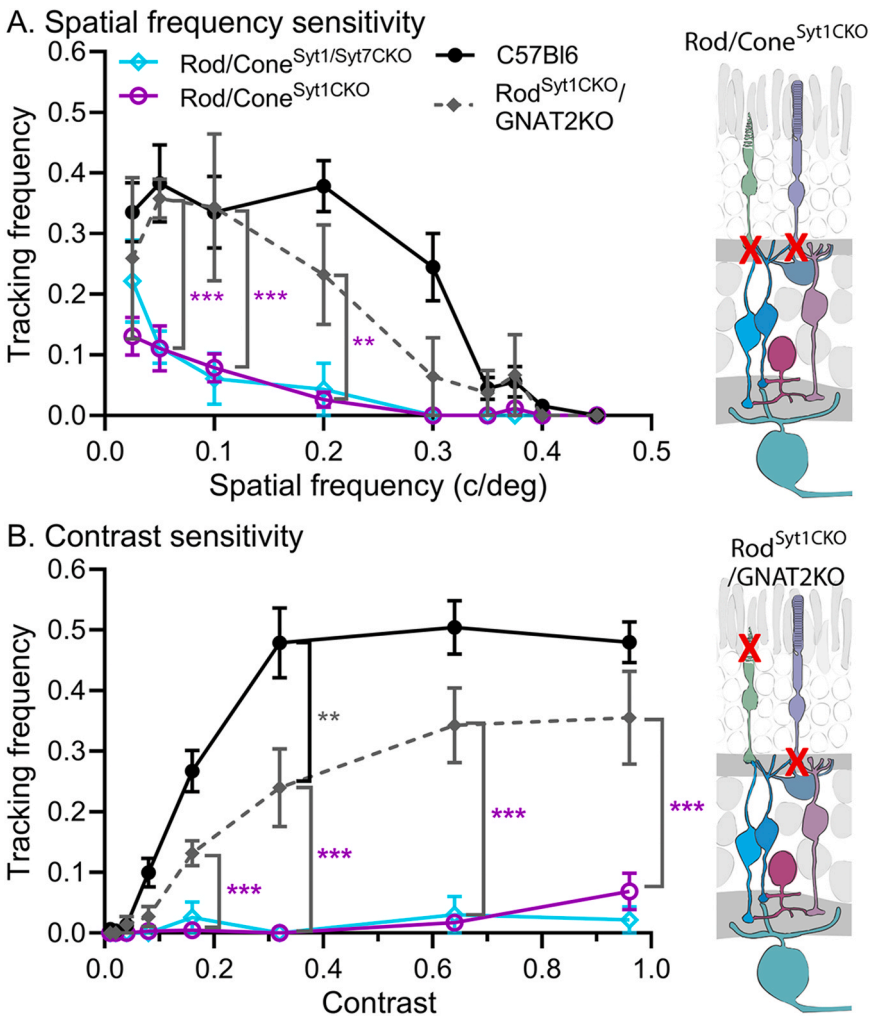

Fig. 4. Optomotor responses of mice with impaired rod and cone inputs. A. Spatial frequency sensitivity. Rod/Cone^{Syt1CKO} mice (n=13) showed a lower frequency of tracking at 0.05c/deg (p=0.012, *), 0.1c/deg (p=0.012, *), 0.2c/deg (p=0.008, **), and 0.3c/deg (<0.0001, ***). Rod^{Syt1CKO}/ GNAT2KO mice also tracked the grating less frequently at 0.05c/deg (p<0.0001, ***), 0.1c/deg (p<0.0001, ***), and 0.2 c/deg (p=0.0013, **). B. Contrast sensitivity. Rod^{Syt1CKO}/GNAT2KO (n=5) mice showed weaker responses than control mice that attained statistical significance at 0.32 contrast (p = 0.0028). Rod/Cone^{Syt1CKO} showed even weaker responses than Rod^{Syt1CKO}/GNAT2KO mice at contrasts of 0.16 (p=0.0003, **), 0.32 (p<0.0001, ***), 0.64 (p<0.0001, ***), and 0.96 (p<0.0001, ***). Video. A. Behavior of C56Bl6J mouse at 1/3 normal speed during a single trial with a high contrast 0.025c/deg grating. B. Behavior of a Rod/Cone^{Syt1CKO} mouse with the same stimulus (video sequence at 1/3 normal speed). This mouse showed an episode of fixation and apparent tracking beginning at 1:05. C. Short segment at normal speed of this same apparent tracking behavior in the Rod/Cone^{Syt1CKO} mouse. The same segment is then shown in reverse and repeated a second time in both forward and reverse directions.

study described in this article and preparation of the article.

Data Availability

The data used to support findings of this study are available from the corresponding author upon request.

Appendix A. Supporting information

Supplementary data associated with this article can be found in the online version at doi:10.1016/j.ibneur.2024.07.003.

References

Abdeljalil, J., Hamid, M., Abdel-Mouttalib, O., Stephane, R., Raymond, R., Auwerx, J., Sahel, J., Chambon, P., Picaud, S., 2005. The optomotor response: a robust first-line visual screening method for mice. Vis. Res *45*, 1439–1446.

Allen, A.E., Storchi, R., Martial, F.P., Bedford, R.A., Lucas, R.J., 2017. Melanopsin contributions to the representation of images in the early visual system. Curr. Biol. *27*, 1623–1632 e1624.

Aranda, M.L., Schmidt, T.M., 2021. Diversity of intrinsically photosensitive retinal ganglion cells: circuits and functions. Cell Mol. Life Sci. *78*, 889–907.

Aung, M.H., Hogan, K., Mazade, R.E., Park, H.N., Sidhu, C.S., Iuvone, P.M., Pardue, M.T., 2022. ON than OFF pathway disruption leads to greater deficits in visual function and retinal dopamine signaling. Exp. Eye Res *220*, 109091.

Brown, T.M., Tsujimura, S., Allen, A.E., Wynne, J., Bedford, R., Vickery, G., Vugler, A., Lucas, R.J., 2012. Melanopsin-based brightness discrimination in mice and humans. Curr. Biol. *22*, 1134–1141.

Delwig, A., Larsen, D.D., Yasumura, D., Yang, C.F., Shah, N.M., Copenhagen, D.R., 2016. Retinofugal projections from melanopsin-expressing retinal ganglion cells revealed by intraocular injections of cre-dependent virus. PLoS One *11*, e0149501.

Doyle, S.E., Grace, M.S., McIvor, W., Menaker, M., 2002. Circadian rhythms of dopamine in mouse retina: the role of melatonin. Vis. Neurosci. *19*, 593–601.

Ecker, J.L., Dumitrescu, O.N., Wong, K.Y., Alam, N.M., Chen, S.K., LeGates, T., Renna, J. M., Prusky, G.T., Berson, D.M., Hattar, S., 2010. Melanopsin-expressing retinal ganglion-cell photoreceptors: cellular diversity and role in pattern vision. Neuron *67*, 49–60.

Fain, G., Sampath, A.P., 2018. Rod and cone interactions in the retina. F1000Res *7*, 657.

Flood, M.D., Veloz, H.L.B., Hattar, S., Carvalho-de-Souza, J.L., 2022. Robust visual cortex evoked potentials (VEP) in Gnat1 and Gnat2 knockout mice. Front Cell Neurosci. *16*, 1090037.

Gooley, J.J., Lu, J., Fischer, D., Saper, C.B., 2003. A broad role for melanopsin in nonvisual photoreception. J. Neurosci. *23*, 7093–7106.

Grassmeyer, J.J., Cahill, A.L., Hays, C.L., Barta, C., Quadros, R.M., Gurumurthy, C.B., Thoreson, W.B., 2019. Ca(2+) sensor synaptotagmin-1 mediates exocytosis in mammalian photoreceptors. Elife *8*, 45946.
Grimes, W.N., Songco-Aguas, A., Rieke, F., 2018. Parallel processing of rod and cone signals: retinal function and human perception. Annu Rev. Vis. Sci. *4*, 123–141.
Jin, N., Tian, L.M., Fahrenfort, I., Zhang, Z., Postma, F., Paul, D.L., Massey, S.C., Ribelayga, C.P., 2022. Genetic elimination of rod/cone coupling reveals the contribution of the secondary rod pathway to the retinal output. Sci. Adv. *8*, eabm4491.
Jin, N.G., Ribelayga, C.P., 2016. Direct evidence for daily plasticity of electrical coupling between rod photoreceptors in the mammalian retina. J. Neurosci. *36*, 178–184.
Kretschmer, F., Tariq, M., Chatila, W., Wu, B., Badea, T.C., 2017. Comparison of optomotor and optokinetic reflexes in mice. J. Neurophysiol. *118*, 300–316.
Le, Y.Z., Ash, J.D., Al-Ubaidi, M.R., Chen, Y., Ma, J.X., Anderson, R.E., 2004. Targeted expression of Cre recombinase to cone photoreceptors in transgenic mice. Mol. Vis. *10*, 1011–1018.
Leinonen, H., Tanila, H., 2018. Vision in laboratory rodents-Tools to measure it and implications for behavioral research. Behav. Brain Res *352*, 172–182.
Li, S., Chen, D., Sauve, Y., McCandless, J., Chen, Y.J., Chen, C.K., 2005. Rhodopsin-iCre transgenic mouse line for Cre-mediated rod-specific gene targeting. Genesis *41*, 73–80.
Lucas, R.J., Allen, A.E., Milosavljevic, N., Storchi, R., Woelders, T., 2020. Can we see with melanopsin? Annu Rev. Vis. Sci. *6*, 453–468.
Mesnard, C.S., Hays, C.L., Barta, C.L., Sladek, A.L., Grassmeyer, J.J., Hinz, K.K., Quadros, R.M., Gurumurthy, C.B., Thoreson, W.B., 2022. Synaptotagmins 1 and 7 in vesicle release from rods of mouse retina. Exp. Eye Res *225*, 109279.
Milla-Navarro, S., Pazo-Gonzalez, M., Germain, F., de la Villa, P., 2022. Phenotype characterization of a mice genetic model of absolute blindness. Int J. Mol. Sci. *23*.
Orhan, E., Neuille, M., de Sousa Dias, M., Pugliese, T., Michiels, C., Condroyer, C., Antonio, A., Sahel, J.A., Audo, I., Zeitz, C., 2021. A new mouse model for complete congenital stationary night blindness due to Gpr179 deficiency. Int J. Mol. Sci. *22*.
Oyster, C.W., Simpson, J.I., Takahashi, E.S., Soodak, R.E., 1980. Retinal ganglion cells projecting to the rabbit accessory optic system. J. Comp. Neurol. *190*, 49–61.
Oyster, C.W., Takahashi, E., Collewijn, H., 1972. Direction-selective retinal ganglion cells and control of optokinetic nystagmus in the rabbit. Vis. Res *12*, 183–193.
Pasquale, R., Umino, Y., Solessio, E., 2020. Rod photoreceptors signal fast changes in daylight levels using a cx36-independent retinal pathway in mouse. J. Neurosci. *40*, 796–810.
Pinto, L.H., Vitaterna, M.H., Shimomura, K., Siepka, S.M., Balannik, V., McDearmon, E. L., Omura, C., Lumayag, S., Invergo, B.M., Glawe, B., et al., 2007. Generation, identification and functional characterization of the nob4 mutation of Grm6 in the mouse. Vis. Neurosci. *24*, 111–123.
Procyk, C.A., Eleftheriou, C.G., Storchi, R., Allen, A.E., Milosavljevic, N., Brown, T.M., Lucas, R.J., 2015. Spatial receptive fields in the retina and dorsal lateral geniculate nucleus of mice lacking rods and cones. J. Neurophysiol. *114*, 1321–1330.
Prusky, G.T., Alam, N.M., Beekman, S., Douglas, R.M., 2004. Rapid quantification of adult and developing mouse spatial vision using a virtual optomotor system. Invest Ophthalmol. Vis. Sci. *45*, 4611–4616.
Quadros, R.M., Miura, H., Harms, D.W., Akatsuka, H., Sato, T., Aida, T., Redder, R., Richardson, G.P., Inagaki, Y., Sakai, D., et al., 2017. Easi-CRISPR: a robust method for one-step generation of mice carrying conditional and insertion alleles using long ssDNA donors and CRISPR ribonucleoproteins. Genome Biol. *18*, 92.
Robinson, D.A., 2022. Neurophysiology of the optokinetic system. Prog. Brain Res *267* 251–269.
Ronning, K.E., Allina, G.P., Miller, E.B., Zawadzki, R.J., Pugh Jr., E.N., Herrmann, R., Burns, M.E., 2018. Loss of cone function without degeneration in a novel Gnat2 knock-out mouse. Exp. Eye Res *171*, 111–118.
Schmucker, C., Seeliger, M., Humphries, P., Biel, M., Schaeffel, F., 2005. Grating acuity at different luminances in wild-type mice and in mice lacking rod or cone function. Invest Ophthalmol. Vis. Sci. *46*, 398–407.
Schroeder, M.M., Harrison, K.R., Jaeckel, E.R., Berger, H.N., Zhao, X., Flannery, M.P., St, Pierre, E.C., Pateqi, N., Jachimska, A., Chervenak, A.P., et al., 2018. The roles of rods, cones, and melanopsin in photoresponses of m4 intrinsically photosensitive retinal ganglion cells (ipRGCs) and optokinetic visual behavior. Front Cell Neurosci. *12*, 203.
Sladek, A.L., Thoreson, W.B., 2023. Using optogenetics to dissect rod inputs to OFF ganglion cells in the mouse retina. Front Ophthalmol. *3*, 1146785.
Umino, Y., Solessio, E., Barlow, R.B., 2008. Speed, spatial, and temporal tuning of rod and cone vision in mouse. J. Neurosci. *28*, 189–198.
Walch, O.J., Zhang, L.S., Reifler, A.N., Dolikian, M.E., Forger, D.B., Wong, K.Y., 2015. Characterizing and modeling the intrinsic light response of rat ganglion-cell photoreceptors. J. Neurophysiol. *114*, 2955–2966.
Zele, A.J., Cao, D., 2014. Vision under mesopic and scotopic illumination. Front Psychol. *5*, 1594.
Zhao, X., Stafford, B.K., Godin, A.L., King, W.M., Wong, K.Y., 2014. Photoresponse diversity among the five types of intrinsically photosensitive retinal ganglion cells. J. Physiol. *592*, 1619–1636.